Breakup of bubbles and drops in steadily sheared foams and concentrated emulsions

K. Golemanov,[1] S. Tcholakova,[1] N. D. Denkov,[1,*] K. P. Ananthapadmanabhan,[2] and A. Lips[2]
[1]*Laboratory of Chemical Physics & Engineering, Faculty of Chemistry, Sofia University, 1 James Bourchier Avenue, 1164 Sofia, Bulgaria*
[2]*Unilever Global Research Center, Trumbull, Connecticut 06611, USA*
(Received 23 May 2008; published 24 November 2008)

This experimental study is focused on the process of bubble breakup in steadily sheared foams, at constant shear rate or constant shear stress. Two different types of surfactants were used and glycerol was added to the aqueous phase, to check how the bubble breakup depends on the surface modulus and on bulk viscosity of the foaming solutions. The experiments show that bubble breakup in foams occurs above a well defined critical dimensionless stress, $\tilde{\tau}_{CR} \equiv (\tau_{CR} R/\sigma) \approx 0.40$, which is independent of surfactant used, solution viscosity, and bubble volume fraction (varied between 92 and 98 %). Here τ_{CR} is the dimensional shear stress, above which a bubble with radius R and surface tension σ would break in sheared foam. The value of the critical stress experimentally found by us $\tilde{\tau}_{CR} \approx 0.40$, is about two orders of magnitude lower than the critical stress for breakup of single bubbles in sheared Newtonian liquids, $\tilde{\tau}_{CR} \approx 25$. This large difference in the critical stress is explained by the strong interaction between neighboring bubbles in densely populated foams, which facilitates bubble subdivision into smaller bubbles. A strong effect of bubble polydispersity on the kinetics of bubble breakup (at similar mean bubble size) was observed and explained. Experiments were also performed with hexadecane-in-water emulsions of drop volume fraction $83\% \leqslant \Phi \leqslant 95\%$ to study drop breakup in concentrated emulsions. Qualitatively similar behavior was observed to that of foams, with the critical dimensionless stress for drop breakup being lower, $\tilde{\tau}_{CR} \approx 0.15$, and practically independent of the drop volume fraction and viscosity ratio (varied between 0.01 and 1). This critical stress is by several times lower than the critical stress for breakage of single drops in sheared Newtonian fluids at comparable viscosity ratio, which evidences for facilitated drop subdivision in concentrated emulsions. To explain the measured low values of the critical stress, a different type of capillary instability of the breaking bubbles and drops in concentrated foams and emulsions is proposed and discussed.

DOI: 10.1103/PhysRevE.78.051405 PACS number(s): 83.80.Iz, 47.57.Bc, 82.70.Kj, 82.70.Rr

I. INTRODUCTION

The typical process of foam generation in the presence of surfactants consists of two subprocesses: air entrapment and bubble breakup. Air entrapment determines the air volume fraction in the generated foam, Φ, whereas the bubble breakup determines the size distribution of the formed bubbles. The bubble size strongly affects all foam properties (such as rheological and optical properties [1–3]), and the foam stability with respect to water drainage, bubble-bubble coalescence, and Ostwald ripening [3–8]. Therefore the mean bubble size and bubble size distribution are among the key factors in all foam applications.

Two qualitatively different regimes of bubble breakup in foams are distinguished. In turbulent flow, bubble deformation in aerated liquids occurs under the action of pressure fluctuations, created by irregular fluid velocity [9–12]. The viscosity of the external phase is of secondary importance in this regime, because the inertial stress deforming the bubbles is of nonviscous origin [9,10]. In contrast, bubble deformation and breakup in regular flows (shear, elongational, etc.) is due to viscous stresses, created by velocity gradients in the continuous phase. In this case, the viscosity of the external phase is an important factor for the efficiency of bubble breakup. The focus of the current study is on the bubble breakup in sheared foams with high gas volume fraction, $\Phi > 74$ vol. %, for which the interactions between the neighboring bubbles are significant and the viscous stress is dominant.

Despite its importance for practice, the process of bubble breakup in sheared foams is still poorly understood in comparison with the process of drop breakup in emulsions [13–17]. Two main reasons for this scarcity of scientific understanding can be pointed out: First, the high volume fraction of the internal phase in foams leads to very strong and poorly understood dynamic interactions between the bubbles. The size distribution after bubble breakup in foams is strongly affected by these interactions, which makes it difficult (or even impossible) to transfer the knowledge from experiments with single bubbles [18–25] to the actual process of bubble breakup in foams. Second, the dynamic viscosity of the internal gas phase in foams is very low—as a result, the bubble deformation under the action of the viscous stress from the external phase does not immediately lead to bubble breakup. The sheared bubbles form elongated threads and additional external perturbations, change in flow conditions, or specific surfactant-related effects are needed to induce bubble breakage [18–25]. From this viewpoint, the analysis of drop deformation and breakage seems easier, because the stress from the continuous phase is transferred to the drop interior mainly through bulk viscous stresses, which induce capillary instability with subsequent drop breakage. These viscous stresses are much better understood both theoretically and experimentally [18–22,26–33].

The major aim of the present study is to clarify the main factors, which control bubble breakup in steadily sheared

*Corresponding author.

 ©2008 The American Physical Society

foams. For this purpose we performed systematic experiments on foams with gas volume fraction, $92 \leqslant \Phi \leqslant 98\%$, which were subject to controlled shear stress or controlled shear rate between the parallel plates of a rheometer. The bubble size distributions before and after the foam shear were determined, and the relation between bubble size, bubble breakup efficiency, and foam rheological properties was analyzed.

Two different surfactant compositions were used as foam stabilizers: synthetic surfactant cocoamidopropyl betaine (CAPB) and a mixture of potassium salts of carboxylic acids (called, for brevity, "soap"). The exact composition of the used foaming solutions is described in Sec. III A. These surfactants were chosen because their solutions exhibit different surface dilatational modulus—very high surface modulus for the soap solutions, $E_S > 300$ mN/m, and low surface modulus for CAPB, $E_S < 5$ mN/m (measured with the oscillating drop method at relatively low frequency, 0.125 Hz, and small amplitudes, $\approx 1\%$, as explained in Ref. [34]). As a result, the stress transfer between the viscous external fluid and the bubble surface is very different for the foams stabilized by these surfactants and hence the rheological properties of the respective foams are also rather different—the shear stress for soap-stabilized foams is higher in comparison with CAPB-stabilized foams, under otherwise similar conditions (see Ref. [34] and Fig. 9 below).

Beside the experiments with foams, we performed measurements with hexadecane-in-water emulsions, allowing us to compare bubble breakup in foams with drop breakup in sheared concentrated emulsions, under similar hydrodynamic conditions. Some nontrivial results about the effect of viscosity ratio on the drop breakup efficiency in sheared emulsions were obtained and are discussed below.

The paper is organized as follows: To facilitate the comparison between foams and emulsions and to create a basis for the discussion of our experimental results, in Sec. II we briefly summarize the main conclusions from previous studies on drop breakup in sheared liquids or emulsions [13–33]. In Sec. III we describe the materials and methods used in our study. In Sec. IV we present and discuss our experimental results, obtained with foams and emulsions. Section V summarizes the conclusions.

II. BACKGROUND—DROP BREAKUP IN SHEAR FLOW

The deformation and breakup of isolated drops, subject to shear flow in viscous fluids, was extensively studied theoretically [18–21,31,33] and experimentally [18,19,26–30,32,35–38]. Starting from the pioneering work of Taylor [26], it was demonstrated that the drop breakup occurs when the capillary number $\mathrm{Ca} = \eta_C \dot{\gamma} R / \sigma$ (which expresses the ratio of the viscous stress acting on the drop surface and drop capillary pressure), exceeds some critical value, $\mathrm{Ca}_{\mathrm{CR}}$, which depends on the ratio of the viscosities of the dispersed and continuous phases, $\lambda = \eta_D / \eta_C$ (called "viscosity ratio"). As usual, σ denotes the interfacial tension and $\dot{\gamma}$ is the shear rate. The experimental works of Grace [22] and Bentley and Leal [28,29] revealed that $\mathrm{Ca}_{\mathrm{CR}}$ depends also on the type of flow—simple shear, hyperbolic, elongational, etc. The drop breakup is affected also by sudden changes in the flow conditions (e.g., of the shear rate), and these time-dependent effects were studied in detail by Stone and Leal [30–33]. Numerical simulations and optical observations of the shape of deformed drops showed that various modes of breakup are possible, such as Rayleigh instability, tip streaming, and end pinching. For comprehensive reviews on this subject one can refer to Refs. [18,19].

One of the main conclusions from the studies with single drops (and bubbles) is that the drop breakup becomes very difficult when the viscosity ratio is low, $\lambda \ll 1$, because the drops and bubbles strongly deform, forming long treads, without rupturing. For example, theoretical and experimental studies showed that the breakup of an isolated bubble in simple shear flow could occur only if $\mathrm{Ca} > 10$ [18–22]. Thus additional perturbations, such as changes in flow conditions, are needed to induce shape instability and drop and bubble breakup for low values of λ.

In several papers it was demonstrated that the main results from the single-drop studies could be extended to drop breakup in emulsions with low and moderate drop volume fraction ($\Phi \leqslant 0.70$) after a simple modification of the approach. Namely, the viscosity of the continuous phase, η_C, is replaced by the emulsion viscosity η_{EM} (at the respective shear rate, $\dot{\gamma}$), i.e., one uses $\mathrm{Ca} = \eta_{\mathrm{EM}} \dot{\gamma} R / \sigma$ and $\lambda = \eta_D / \eta_{\mathrm{EM}}$ in the system description. Thus experiments in Ref. [15] showed that the dependence $\mathrm{Ca}_{\mathrm{CR}}(\lambda)$ for a series of emulsions with $\Phi \leqslant 0.70$ is similar to that for isolated drops, when using η_{EM} instead of η_C (see Fig. 7 below for results). Therefore, in such diluted emulsions, the effect of interdroplet interactions on drop breakup can be accounted for by the so-called "effective medium approach" [15,39].

Drop breakage in more concentrated emulsions (volume fraction above the sphere close-packing, $\Phi > 74\%$) was studied by Bibette *et al.* [13,14,16,40]. These authors showed that monodisperse emulsions could be formed by simple shear under appropriate conditions [40], which include (i) the narrow gap of the shear cell, and (ii) the viscosity ratio close to unity. Similar conditions for obtaining monodisperse drops in more diluted emulsions with $\Phi < 70\%$ were reported recently in Ref. [17]. Bibette and co-authors showed also that the size of the formed drops depends mostly on the shear rate, interfacial tension, and viscosity ratio. Noticeably, the experiments with concentrated emulsions demonstrated [16] that drop breakup in shear flow could occur even when the viscosity ratio is much higher than unity (up to $\lambda \approx 100$), which is well above the established boundary for the breakup of single drops in a simple shear flow of Newtonian continuous phase ($\lambda \approx 4$). The latter result emphasizes the nontrivial effects of drop-drop interactions and the facilitated drop breakage in concentrated emulsions.

In a recent paper Mabille *et al.* [16] showed that the final mean drop size in concentrated emulsions is determined mainly by the applied shear stress. Interestingly, these authors found a relatively weak effect of the viscosity ratio on the conditions for drop breakup—the critical capillary number $\mathrm{Ca}_{\mathrm{CR}}$ was measured to be ≈ 0.1 for viscosity ratio $\lambda = \eta_D / \eta_C \approx 1$ (while for single drops with similar viscosity ratio $\mathrm{Ca}_{\mathrm{CR}} \approx 0.3$), and decreased slightly to 0.04 with the decrease of λ down to 0.01, which is opposite trend to the prediction for isolated drops.

It is obvious from the above brief literature overview that the conditions for bubble breakup in foams and for drop breakup in concentrated emulsions, with $\Phi > 74\%$, are far from clear, even for the simplest case of steady shear flow. This was the starting point and the main motivation for performing the present study.

III. MATERIALS AND METHODS

A. Materials

Solutions of two different types of surfactant were used for foam generation: (i) 3 wt % cocoamidopropyl betaine (CAPB, commercial name Tego Betaine F50; Goldschmidt Chemical); and (ii) mixed potassium salts of fatty acids, denoted hereafter as "soap solution."

The soap solution was prepared by dissolving 0.45 wt % Lauric acid, 0.9 wt % Myristic acid, 0.5 wt % Palmitic acid, 0.1 wt % Stearic acid, and 0.5 wt % KOH in pure water (or in a mixture of water and glycerol), upon heating at 50 °C. The obtained clear solution was left to cool down and its *p*H was adjusted to 10.1 ± 0.1 by addition of small aliquots of 0.1 M HCl solution. During this *p*H adjustment, solid particles of precipitated soap were formed. Therefore the soap solutions were centrifuged for 30 min at 4000 g, just before the actual experiments, to remove the solid particles and to obtain clear foaming solution. The surfactants and their concentrations were chosen to ensure Newtonian behavior of the foaming solution.

For emulsion preparation we used hexadecane as oil phase (product of Merck) and 3 wt % solution of the nonionic surfactant polyoxyethelene-8 tridecyl ether (C13EO8, product of Rhodia, trade name ROX) as the aqueous phase. This surfactant was chosen because it ensures high emulsion stability against drop-drop coalescence and Newtonian behavior of the aqueous phase.

All surfactant solutions were prepared with deionized water, purified with the Millipore Organex Q system. For most experiments, glycerol was added to the aqueous phase, in concentration up to 60 wt %, to vary solution viscosity. The properties of all solutions are summarized in Table I.

B. Measurements of bulk viscosity and surface tension of the foaming solutions

Viscosity of surfactant solutions, η_C, was measured with a thermostated capillary viscometer. These solutions were tested also for possible shear thinning by running rheological measurements (steady shear) on a Gemini model research rheometer (Bohlin and Malvern Instruments, UK) in the range of shear rates between 0.1 and 150 s^{-1}. No detectable dependence of solution viscosity on the shear rate was found and therefore surfactant solutions were considered as Newtonian liquids.

The surface tension of the foaming solutions and hexadecane-water interfacial tension was measured by drop-shape analysis of pendant drops. These measurements were performed on a DSA100 apparatus (Krüss, Germany) at 25.0 ± 0.5 °C, and the obtained results are shown in Table I.

TABLE I. Properties of the surfactant solutions used ($T = 25$ °C).

Surfactant	Glycerol concentration (wt %)	Viscosity, η_C (mPa s)	Surface tension, σ (mN/m)
3 wt % CAPB	30	2.59	30.4
	40	3.75	30.2
	60	11.4	30.2
K carboxylate, *p*H=10.1	0	0.895	22.6
	30	2.12	26.7
	40	3.19	27.0
3 wt % ROX	0	1.41	1.5[a]
	30	4.75	1.3[a]

[a]Interfacial tension of hexadecane-solution interface.

C. Generation of initial foam for bubble breakup experiments

The initial foams for the bubble breakup experiments were usually generated in a glass cylinder, by blowing nitrogen gas through a set of glass capillaries, mounted at the cylinder bottom and immersed in the surfactant solution [41]. Foams generated by this procedure contained relatively monodisperse large bubbles with mean volume-surface radius $R_{32} \approx 800 \pm 100$ μm.

To study the effect of foam polydispersity on the bubble breakup process, in some of the experiments we used polydisperse foam, prepared by a series of ejection and injection cycles of the foam through a syringe needle, as described in Ref. [34]. Slow ejection and injection speed was used, resulting in mean bubble radius, $R_{32} \approx 950$ μm, and relatively wide width of the size distribution, ± 230 μm.

D. Preparation of initial emulsions for drop breakup experiments

Initial hexadecane-in-water emulsions, containing relatively large monodisperse oil drops, were prepared by membrane emulsification. In this method, the dispersed phase (hexadecane in our experiments) is emulsified by passing it through membrane pores, under pressure, into the surfactant solution [42,43]. We used a laboratory Microkit membrane emulsification module from Shirasu Porous Glass Technology (SPG, Japan), which works with tubular glass membranes of outer diameter 10 mm and working area of approximately 35 cm^2. Membranes with mean pore size of 7 μm were used for preparing the initial emulsions, which contained monodisperse drops with radius $R_{32} \approx 12 \pm 1$ μm. These emulsions were concentrated for the drop breakup experiments, by centrifugation at 20 g for 1 h, and subsequent removal of the separated aqueous phase, which did not contain oily drops. In this way we were able to prepare series of initial emulsions with similar drop radius and different oil volume fractions.

E. Determination of the bubble and drop size distribution and of the average bubble and drop size

Bubble size distribution in the foams was determined before and after the bubble breakup experiments, by using the procedure of Garrett *et al.* [44]. In this method, about 1 mL foam is spread as a thick layer on the base wall of a triangular prism. Images of the wetting films, formed in the zone of contact of the foam with the prism, are taken by a video camera, equipped with a long-focus magnifying lens. These films are illuminated by diffuse white light through one of the side walls of the prism, whereas the film observation is made through the other side wall of the prism. The images are processed by free software ImageJ 1.36b, released by the National Institute of Health (NIH) [45], to determine the area occupied by each bubble on the wall surface. The distribution of the areas, occupied by the bubbles, is transformed into bubble size-distribution histogram as described in Ref. [44], and the mean volume-surface radius R_{32} is determined.

The drop size distribution in the studied emulsions (before and after drop breakup experiments) was determined by video-enhanced optical microscopy [46,47]. The oil drops were observed and recorded in transmitted light with microscope Axioplan (Zeiss, Germany), equipped with objective Epiplan ×50, and connected to a charge-coupled device (CCD) camera and video recorder. The diameters of the recorded oil drops were measured one by one, using custom-made image analysis software, operating with Targa +graphic board (Truevision, USA). For each sample, the diameters of at least 1000 drops were measured. The accuracy of optical measurements was estimated to be ± 0.3 μm [46].

F. Bubble (drop) breakup in shear flow and rheological characterization of the obtained foams (emulsions)

These experiments were performed in two consecutive stages: (stage 1) Bubble breakup in the rheometer, at fixed shear rate or shear stress, and (stage 2) characterization of the rheological properties of the foam, which is obtained after stage 1. The shear rate during stage 2 (rheological characterization) was lower than the shear rate used during stage 1, to avoid the possible bubble breakup in stage 2. Bubble size distribution was determined before starting stage 1 and after finishing stage 2. All experiments were performed at 25 °C.

The specific procedure for performing these experiments was the following:

The initial foam, containing relatively large bubbles, was placed between two parallel plates in the Gemini rotational rheometer (Bohlin and Malvern Instruments, UK); see Fig. 1. Sandpaper of type P100 or P40 was glued on both plates to reduce or eliminate foam-wall slip. The radius of the parallel plates was 20 mm and the gap between them was set at 3 mm.

During stage 1, the foam was sheared at fixed shear rate or fixed shear stress—the resulting shear stress (or shear rate) was recorded as a function of time. During this stage, the bubbles broke down, and the bubble size distribution at the end of the experiment depended on the applied shear rate (stress) and on the duration of shearing. The process of bubble breakup was reflected in an increase of the measured shear stress (at fixed rate) or decrease of the shear rate (at fixed stress), because the stress of sheared foam is inversely proportional to the mean bubble size of certain power [1].

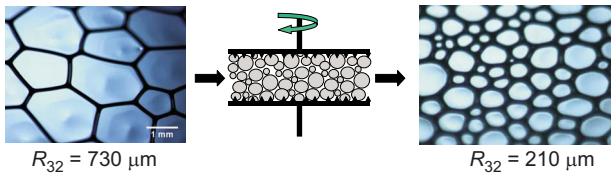

FIG. 1. (Color online) Breakup of bubbles in sheared foam. The initial foam, containing relatively large bubbles, is placed between the parallel plates in rotational rheometer (B). The plate radius is 2 cm and the gap between the plates is 3 mm. Sandpaper is glued on the plates to reduce the foam-wall slip. The foam is sheared at fixed shear rate or fixed shear stress. The resulting shear stress (or shear rate) is recorded as a function of time. The bubble size distribution before (A) and after (C) foam shearing is determined by optical observations and image analysis, as explained in Sec. III E. Note that these images are taken after deposition of the studied foam as a thick layer on the wall of triangular optical prism—under these conditions, water drainage from the foam in contact with the prism wall is possible, which explains the visual difference in the air volume fraction for the images taken before and after bubble breakup.

During stage 2, the foam was sheared in steps from high to low shear rates to characterize foam rheological properties. At each shear rate, 2 sec delay time and 3 sec integration time were used to measure the shear stress (independent experimental checks showed that these times were sufficiently long to provide correct data). The obtained curves "shear stress vs shear rate," were fitted by Herschel-Bulkley model,

$$\tau = \tau_0 + k\dot{\gamma}^n, \tag{1}$$

and the rheological characteristics of the foam were determined: yield stress τ_0, consistency k, and power-law index n.

The experiments with emulsions were performed by using the same procedure, with the only exception that the glued sandpaper was of type P150 (finer grains) and the gap between the parallel plates was varied between 0.3 and 0.5 mm. The results from the rheological experiments with emulsions were independent of the gap (for a given system), which was a clear indication that these experiments were not affected by wall slip.

We note that in the experiments with foams, we could not entirely suppress the wall slip in the beginning of the experiment, when the bubbles were relatively large (the measurements showed that the measured shear stress, at given shear rate, was dependent on the gap between the plates). Therefore the quoted shear rates in the bubble breakup experiments (during stage 1) should be considered as "apparent" shear rates. For this reason, all final results and conclusions related to the bubble breakup process are expressed in terms of the shear stress, which is directly measured by the instrument—thus no assumptions about the presence or absence of wall slip were used to formulate these final results and conclusions.

Note also that all rheological data were recalculated to correspond to the shear rate and stress at the periphery of the parallel plates where the shear rate is maximal. Correspondingly, samples for determination of bubble and drop size distribution were taken only from this periphery zone. Thus the problem with the different shear rates, as one varies the distance from the center of the plates, was avoided.

Another important comment is that we used optical observations (including observations with a high-speed camera) to check for the homogeneity of the foam flow at the periphery of the sample and to observe the process of bubble breakup (see Fig. 8 below). These observations evidenced homogeneous flow of the foam across the gap, without signs for shear banding or any other characteristics of the nonhomogenous flows. Note that the bubble and drop breakup experiments described in the current paper are performed at shear stresses, which are well above the yield stress of the respective system, whereas the nonhomogeneous flows are usually observed at stresses comparable to the yield stress of the system.

IV. EXPERIMENTAL RESULTS AND DISCUSSION

A. Critical stress for bubble and drop breakup

Two types of bubble and drop breakup experiments were performed—at constant shear rate and at constant shear stress. In both types of experiments three qualitatively different scenarios were observed, depending on the applied shear rate and stress:

(i) When the applied shear rate (or stress) is lower than a given value, denoted hereafter as the critical rate $\dot{\gamma}_{CR}$ (or critical stress τ_{CR}), the measured shear stress (rate) remains constant during the entire experiment, see the lowest curve for $\dot{\gamma}=2\ s^{-1}$ in Fig. 2(a). In this case, the initial and the final bubble and drop size distributions are virtually the same—no bubble and drop breakup occurs in these experiments.

(ii) When the applied stress (rate) is around $\dot{\gamma}_{CR}$ (or τ_{CR}), the measured shear stress increases (the shear rate decreases) almost linearly with time—see as an example the curve obtained at $\dot{\gamma}=25\ s^{-1}$ in Fig. 2(a). In these systems, the mean bubble and drop size gradually decreases with time.

(iii) When the applied rate is significantly higher than $\dot{\gamma}_{CR}$ (or τ_{CR}), two well distinguished regions are observed in the experimental curves stress (or rate) vs time—a fast process with a characteristic time scale of several seconds, and a slow process with a characteristic time scale of tens of minutes. During the fast process, the shear stress increases (or the shear rate decreases) by several times within seconds, whereas a much slower change in the measured quantities is observed during the second region—see as examples the two top curves in Fig. 2(a) and the curves in Fig. 3(a). Related significant reduction of the mean bubble and drop size is observed in these experiments.

From the physicochemical viewpoint, it is more appropriate to discuss these results in terms of the shear stress, because this is the driving force for bubble and drop deformation and breakup. Therefore the following discussion is focused on the comparison of the applied shear stress with the bubble and drop capillary pressure.

The actual value of the *dimensional* critical stress τ_{CR} depends on the initial bubble and drop size, interfacial tension, and type of dispersed phase (air or oil). To account for the effects of bubble and drop size and of interfacial tension, we define a size-dependent *dimensionless* critical stress, $\tilde{\tau}_{CR}(R)=\tau_{CR}R/\sigma$, which expresses the ratio between the mean shear stress in the foam and emulsion and the capillary pressure of a given drop and bubble with radius R, that would lead to breakup of the respective drop or bubble. By analysis of the experimental data for all studied foams with $0.92\leqslant\Phi\leqslant 0.98$, $150\leqslant R_{32}\leqslant 1000\ \mu m$, and $1\leqslant\eta_C\leqslant 10$ mPa s, we found that the critical dimensionless stress, above which the bubbles break inside sheared foam, is practically constant, $\tilde{\tau}_{CR}\approx 0.40\pm 0.02$ (determined as statistically averaged value over more than 30 different samples).

The importance of this critical stress is illustrated in Fig. 2(b), where the experimentally measured bubble size distribution (by volume) for the initial foam is presented as a function of the dimensionless stress exerted on the bubbles, $\tilde{\tau}(R)\equiv(\tau R/\sigma)$, at several shear rates. As seen from Fig. 2(b), when the foam is sheared at $\dot{\gamma}=2\ s^{-1}$ [corresponding to $\tau=6$ Pa, cf. with Fig. 2(a)], the dimensionless stress for *all bubbles* in the foam is lower than the critical one, $\tilde{\tau}(R)<\tilde{\tau}_{CR}\approx 0.4$. As a result, no bubble breakup occurs and the bubble size distribution remains the same during foam shear.

In contrast, when similar foam is sheared at $\dot{\gamma}=25\ s^{-1}$, the mean stress increases to $\tau=10$ Pa and hence a small fraction of the largest bubbles in this foam are subject to stress, which is above the critical one; see the curve connecting the full circles in Fig. 2(b). As a result, the biggest bubbles in the initial foam break into smaller bubbles during shearing at $\dot{\gamma}=25\ s^{-1}$ [see Fig. 2(c), where the initial and the final bubble size distributions are compared].

Note that during shearing at $\dot{\gamma}=25\ s^{-1}$ for 300 s, the mean drop radius R_{32} decreases from $\approx$0.9 to 0.5 mm, which results in an increase of the mean shear stress from 10 to 13.5 Pa. Due to this simultaneous change of the mean bubble size and the mean shear stress, the fraction of bubbles, which are subject to dimensionless stress $\tilde{\tau}(R)>\tilde{\tau}_{CR}$ in the foam remains similar to that in the initial foam during the entire shearing process. This observation explains why the slope of the curve $\tau(t)$ remains almost constant, around 0.7 Pa/min, during the entire duration of foam shear at $\dot{\gamma}=25\ s^{-1}$. In addition, these and other similar experiments (see Sec. IV B) evidenced that the dimensionless critical stress $\tilde{\tau}_{CR}$ did not depend on the size of the sheared bubbles, viz. on the number of bubble layers in the gap between the plates.

When the foam is sheared at higher rate, $30\ s^{-1}$, most of the bubbles in the initial foam are subject to stress that is well above the critical one—see the respective curve in Fig. 2(b). As a result, very fast bubble breakup starts at this shear rate immediately after imposing the deformation [see Fig. 2(a)]. Note that the initial process of fast bubble breakup is followed by a second stage of slower bubble breakup. During this second stage, the mean bubble size continues to decrease with time, due to the fact that a noticeable fraction of bubbles still exist (5–10 vol %), which are subject to stress $\tilde{\tau}(R)>\tilde{\tau}_{CR}$.

Similar experiments with the respective data analysis were performed at constant shear stress, as well. In Fig. 3 we

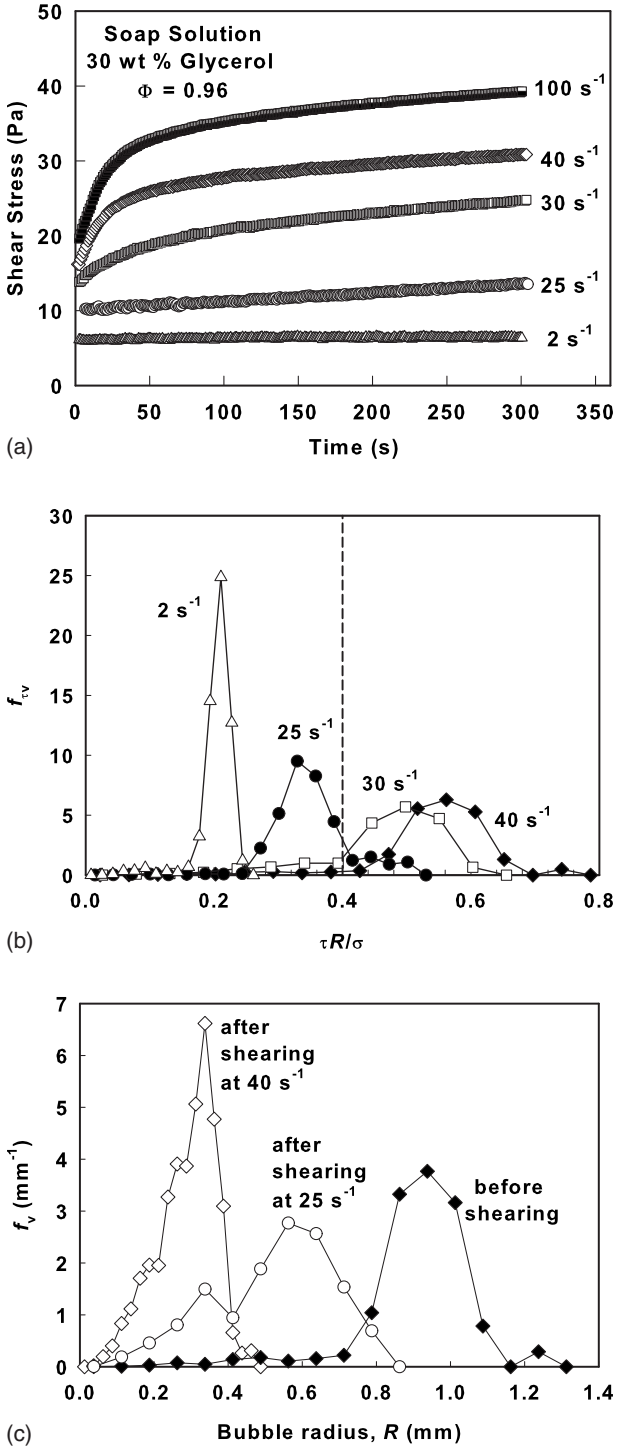

FIG. 2. (a) Shear stress as a function of time for foam stabilized by soap solution +30 wt % glycerol at different shear rates. (b) Bubble distribution by volume, in the initial foam, as a function of the dimensionless shear stress $\tilde{\tau}(R) \equiv (\tau R/\sigma)$, at different shear rates. Note that the different shapes of the curves in this plot come mainly from the different shear rates, applied in the rheological measurements, which lead to different average shear stress τ appearing as a multiplier for the values on the abscissa. (c) Comparison of the bubble size distributions by volume in the initial foam and in the final foams, sheared at $\dot{\gamma}=25\ s^{-1}$ and at $40\ s^{-1}$, respectively.

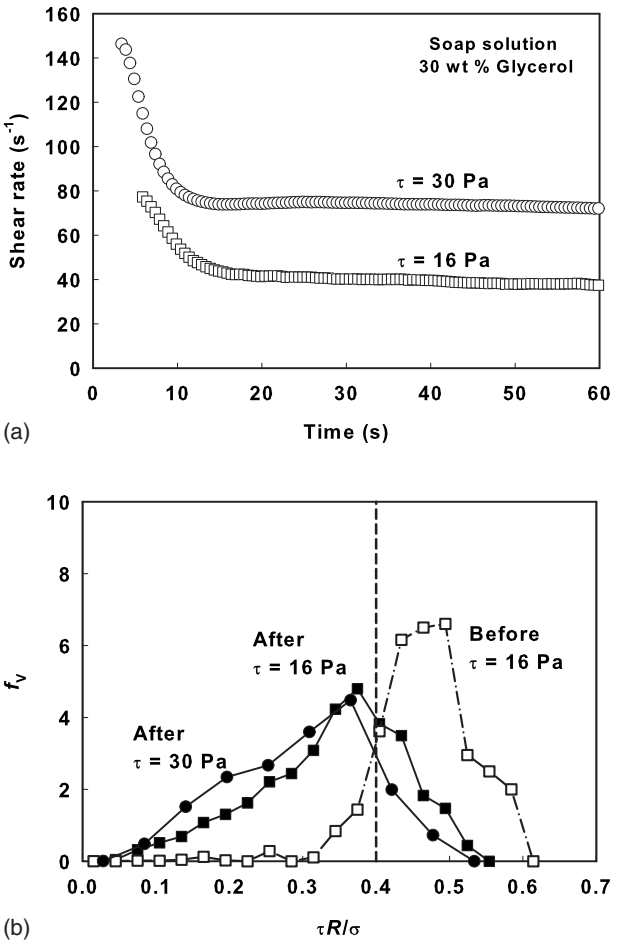

FIG. 3. (a) Shear rate as a function of time for foams stabilized by soap solution +30 wt % glycerol, which are sheared at fixed stress, τ. (b) Bubble distribution by volume, as a function of the dimensionless shear stress $\tilde{\tau}(R) \equiv (\tau R/\sigma)$, of the bubbles in the initial foam (empty squares), and in the final foams, obtained after shearing at 16 Pa (full squares) and at 30 Pa (full circles).

show illustrative results for soap-stabilized foams, sheared at 16 and 30 Pa, respectively. In both experiments, the applied shear stress corresponds to a significant fraction of bubbles in the foam being above $\tilde{\tau}_{CR}$. As a result, fast initial bubble breakup occurs during the first several seconds (evidenced by the rapid decrease of the shear rate), followed by a second stage of gradual slow decrease of bubble size.

As mentioned above, the analysis of all experimental data obtained with CAPB-stabilized and soap-stabilized foams, performed at a constant shear rate or at a constant shear stress, showed that the critical dimensionless stress, required for bubble breakup in sheared foams, is $\tilde{\tau}_{CR} \approx 0.40 \pm 0.02$.

Experiments with hexadecane-in-water emulsions were also performed and showed very similar qualitative trends—see as illustration the results shown in Fig. 4. The main difference between the studied foams and emulsions was that the critical dimensionless stress for drop breakup was $\tilde{\tau}_{CR} \approx 0.15 \pm 0.02$ (determined from experiments with more than 20 different samples), which is almost three times lower than the critical stress for bubble breakup. Further comparison and discussion of the critical stress for foams and emulsions is presented in Secs. IV C and IV D below.

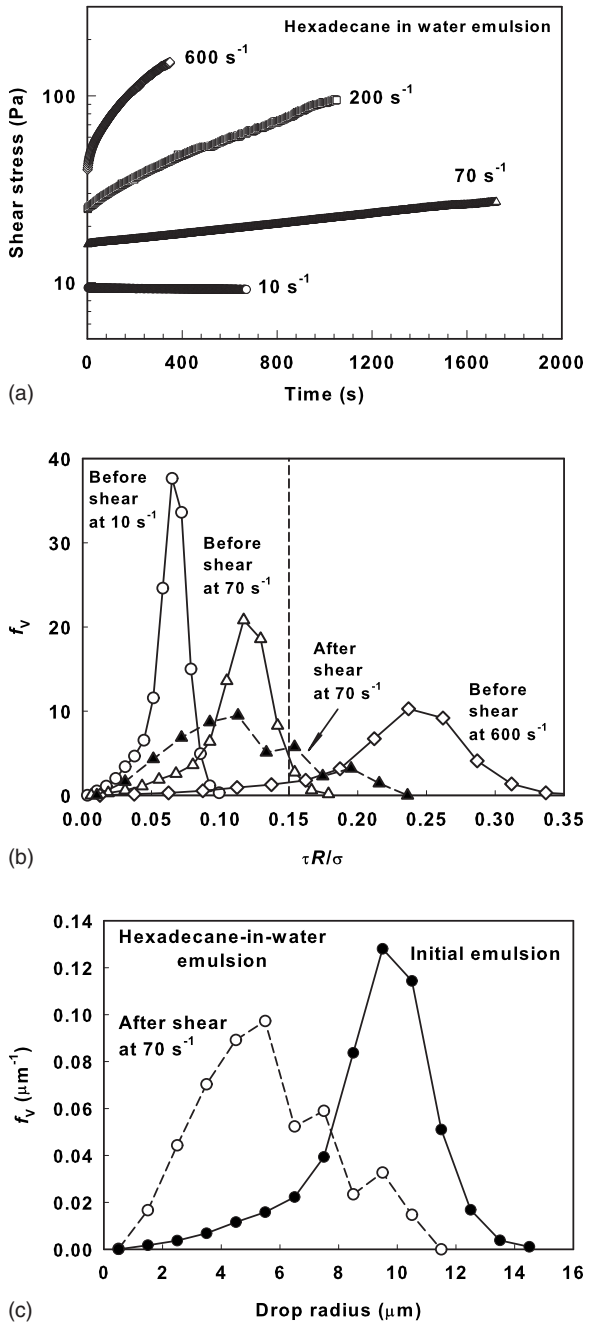

FIG. 4. (a) Shear stress as a function of time for hexadecane-in-water emulsions, stabilized by 3 wt % ROX +30 wt % glycerol, and sheared at different rates. (b) Drop distribution by volume, in the initial emulsion, as a function of the dimensionless shear stress $\tilde{\tau}(R) \equiv (\tau R/\sigma)$, at different shear rates. For comparison, the same distribution for the final emulsion obtained after shearing at 70 s^{-1} is shown by full triangles. (c) Comparison of the drop size distributions by volume in the initial emulsion and in the final emulsion sheared at $\dot{\gamma}=70$ s^{-1}.

B. Effect of foam polydispersity on the bubble breakup process

Our experiments showed that the kinetics of bubble breakup is much faster in polydisperse foams, as compared to foams containing monodisperse bubbles with the same mean radius. This nontrivial relation between kinetics of bubble breakup and foam polydispersity is discussed in the current section.

In Fig. 5 we show experimental results for the kinetics of bubble breakup in CAPB-stabilized foams, containing initially *monodisperse* bubbles, and sheared at a constant shear rate of 100 s^{-1}. As an indicator for the rate of bubble breakup we could use the change in the measured shear stress, Fig. 5(a), because this stress increases with the reduction of bubble size. In addition, we took foam samples and determined the bubble size distribution in four moments along the bubble breakup process—see the points denoted by numbers 1—4 in Fig. 5(a) and the respective size-distribution curves in Fig. 5(b).

As seen from Fig. 5(a), the bubble breakup process occurred in three main stages in these experiments: (i) the initial (induction) period, during which the shear stress and the bubble size changed slowly; (ii) the fast bubble breakup, during which an abrupt increase of the shear stress was observed; (iii) the plateau region of almost constant shear stress and bubble size (in most of the experiments, slow increase of the shear stress and concomitant decrease of the mean bubble size were observed during this third stage).

The analysis of rheological data from these experiments, optical observations of the bubbles in the sheared foam by a high-speed camera, and bubble size-distribution histograms [Fig. 5(b)] provided the following explanation of these three stages:

(i) During the induction period [see the experimental curve between points 1 and 2 in Fig. 5(a)] most of the bubbles in the initial foam are subject to shear stress, which is below the critical one [curve 1 in Fig. 5(b)]. Only a small fraction of the largest bubbles in the initial foam are subject to shear stress above the critical one, and these bubbles occasionally break into smaller bubbles. Thus small bubbles are gradually accumulated in the foam during this induction period, which results in the observed slow increase of the average shear stress of the foam.

(ii) The increase of the shear stress during the induction period leads to a moment, when more than 50% by volume of the bubbles in the foam become subject to a stress, which is above the critical one [see curve 2 in Fig. 5(b)]. This moment, denoted as point 2 in Fig. 5, indicates the end of the induction period and the beginning of the stage of fast bubble breakup. In other words, the small bubbles generated during the induction period increase the stress, which in its own turn induces fast breakup of the bigger bubbles in the foam—thus an "autocatalytic" avalanche cascade of bubble breakup events occurs during the second stage [between points 2 and 3 in Fig. 5(a)]. As a result, the shear stress increases by two to three times and the mean bubble radius decreases from $R_{32} \approx 700$ μm down to $R_{32} \approx 300$ μm within seconds.

(iii) During the third stage [between points 3 and 4 in Fig. 5(a)], the shear stress increases slowly with time. The main fraction of large bubbles has been already broken and the capillary pressure of the formed small bubbles is too high to allow a significant bubble deformation, see curve 4 in Fig. 5(b). There is only a small fraction of big bubbles, which gradually break into smaller bubbles during this stage, which

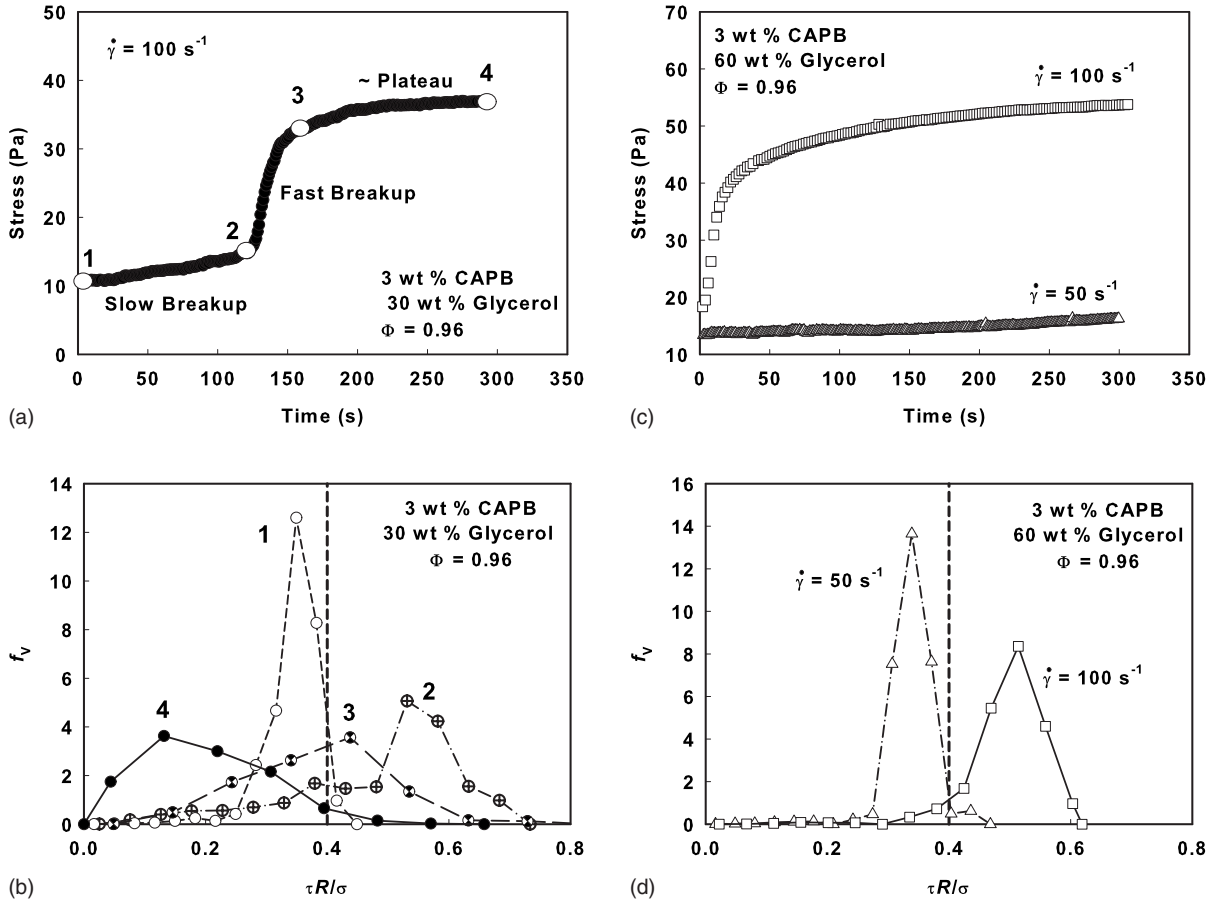

FIG. 5. Shear stress as a function of time for monodisperse foams, stabilized by (a) 3 wt % CAPB +30 wt % glycerol at shear rate of 100 s^{-1} and (c) 3 wt % CAPB +60 wt % glycerol, at shear rates of 50 and 100 s^{-1}. Bubble distribution by volume, as a function of the dimensionless shear stress $\tilde{\tau}(R) \equiv (\tau R/\sigma)$ for the bubbles in (b) points 1–4 in (a), (d) initial foam in (c), subject to shear at 50 and 100 s^{-1}.

explains the observed slow increase of the shear stress.

Very similar results (same stages and related changes in bubble size) were obtained with monodisperse foams, formed from CAPB solutions of higher viscosity [see Figs. 5(c) and 5(d) and Table I].

The kinetics of bubble breakup in *polydisperse* foams was qualitatively different, as illustrated in Fig. 6. Despite the similar mean bubble size in the monodisperse and polydisperse foams shown in Fig. 6 ($R_{32} \approx 950\ \mu$m), the fast breakup process started immediately in the case of the polydisperse foam, whereas a long induction period was observed with the monodisperse foam (at the same shear rate of 100 s^{-1}). These results are easily explained, by considering the size distribution in the two types of foams: More than 50% by volume of the bubbles in the initial polydisperse foam were under shear stress higher than $\tilde{\tau}_{CR}$; see Fig. 6(b). In contrast, only around 5% of the bubbles in the monodisperse foam were subject to stress above the critical one. Interestingly, in the final "plateau" region, the average shear stress and the bubble size distribution in the two types of foams were similar, i.e., the initial polydispersity affects mostly the kinetics of bubble breakup, whereas the final bubble size distribution is similar, cf. the curves in Fig. 6(c) (see Sec. IV D below for further discussion of this point). In this plateau region, only a small fraction of the bubbles are subject to stress higher than $\tilde{\tau}_{CR}$ and, as a result, the bubble breakup process is slow.

We can conclude from all performed experiments that there is a well defined value of the dimensionless shear stress, above which the bubbles and drops in the concentrated foam and emulsions are broken during steady shear deformation. The critical dimensionless stress is around $\tilde{\tau}_{CR} \approx 0.40$ for bubbles in the studied foams, and $\tilde{\tau}_{CR} \approx 0.15$ for the drops in the studied emulsions. The kinetics of bubble and drop breakup is governed by the fraction of bubbles and drops in the foam and emulsion, which are subject to a stress, which is higher than $\tilde{\tau}_{CR}$. Slow breakup is observed when $\approx 5-10$ % of the bubbles and drops (by volume) are subject to stress higher than $\tilde{\tau}_{CR}$. In contrast, rather fast, avalanche-type breakup occurs when more than 50% of the bubbles and drops are subject to stress higher than $\tilde{\tau}_{CR}$.

C. Comparison of conditions for drop breakup in concentrated and diluted emulsions

As mentioned in the introduction, the critical capillary number for breakup of single drops in simple shear flow, Ca_{CR}, depends predominantly on the viscosity ratio of the dispersed and continuous phases. In the classical study by Grace [22], it was shown experimentally that Ca_{CR}

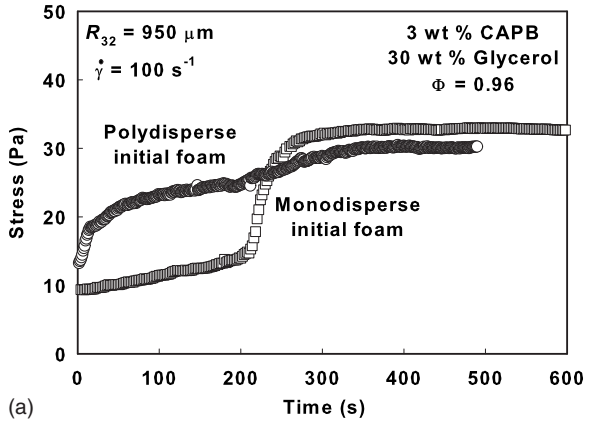

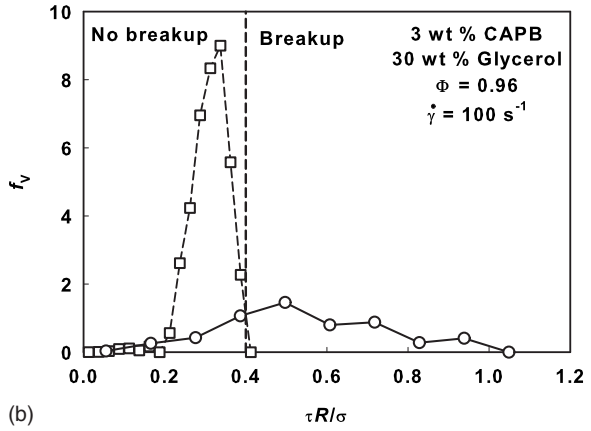

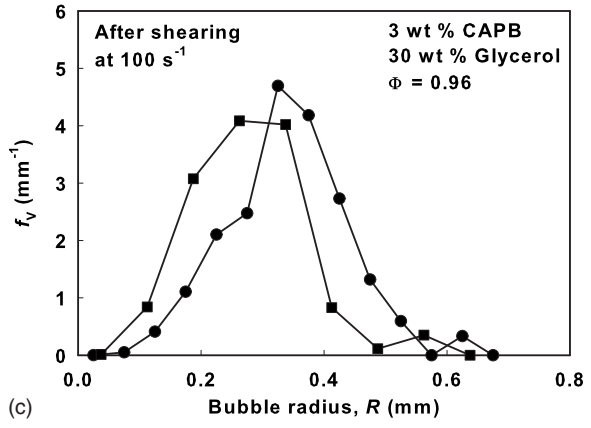

FIG. 6. (a) Shear stress as a function of time for foams stabilized by 3 wt % CAPB +30 wt % glycerol at shear rate of 100 s^{-1} for monodisperse (empty squares) and polydisperse (empty circles) initial foams. (b) Bubble distribution by volume, as a function of the dimensionless shear stress $\tilde{\tau}(R) \equiv (\tau R/\sigma)$, for the bubbles in the initial monodisperse (empty squares) and polydisperse (empty circles) foams. (c) Comparison of the bubble size distributions in the final foams formed from initial monodisperse (full squares) and initial polydisperse (full circles) foams, after shearing at $\dot{\gamma}$ = 100 s^{-1}.

$= \eta_C \dot{\gamma} R/\sigma$ passes through a minimum around $\lambda \approx 1$; see the dashed curve in Fig. 7. The results by Jansen *et al.* [15] showed that this concept could be extended to drop breakup in emulsions with oil volume fraction up to 70%, if the viscosity of the continuous phase η_C is replaced by the emulsion viscosity η_{EM}. In Ref. [15], the viscosity of the continuous phase is defined as $\eta_{EM} = \tau/\dot{\gamma}$, where τ is the measured shear stress and $\dot{\gamma}$ is the shear rate, at which the drop breakup occurs. One sees from this definition of η_{EM} that the critical capillary number for drop breakup in emulsions defined by Jansen *et al.* [15], $Ca_{CR} = \eta_{EM} \dot{\gamma} R/\sigma = \tau_{CR} R/\sigma$, is identical to the dimensionless critical shear stress, as defined by us in the current study, $\tilde{\tau}_{CR} = \tau_{CR} R/\sigma$. Following this analogy, we present below our experimental results for foams and concentrated emulsions in the form of dimensionless critical stress, required for bubble and drop breakup, as a function of the viscosity ratio, $\lambda = \eta_D/\eta_{EM}$ (for diluted emulsions this plot is equivalent to the classical Grace plot). Our experimental data (squares) are compared in Fig. 7 with those obtained by Grace [22] for isolated drops (dashed curve) and by Jansen *et al.* [15] for drops in diluted emulsions (circles).

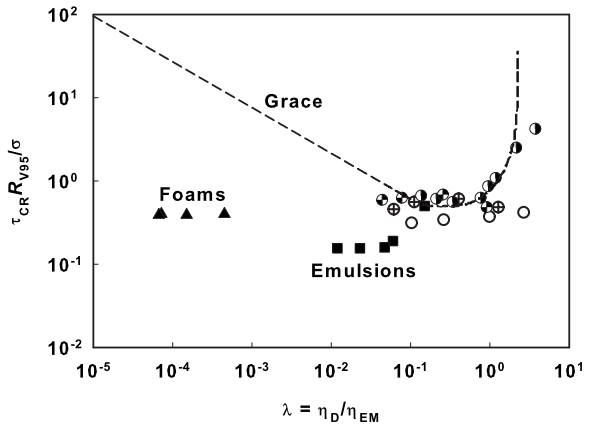

FIG. 7. Dimensionless critical stress for drop and bubble breakup in simple shear flow, as a function of the viscosity ratio λ. The dashed curve represents the experimental data by Grace [22] for isolated drops in shear flow. The circles represent experimental results obtained by Jansen *et al.* [15] for drops in emulsions with oil volume fraction Φ ≤ 70%. The squares represent our experimental results for breaking of drops in concentrated emulsions (Φ > 80%). The triangles represent our experimental results for breaking of bubbles in concentrated foams (Φ > 92%).

One sees that the dimensionless critical stress for the studied *concentrated* emulsions, $\tilde{\tau}_{CR} \approx 0.15$ (corresponding to a critical capillary number $Ca_{CR} \approx 0.15$), is much lower than Ca_{CR} for single drops, and does not depend on the viscosity ratio in the studied range between 10^{-2} and 0.5 (similar experimental results were reported in Ref. [16]). Note that in the range of low viscosity ratios, $\lambda \sim 10^{-2}$, the critical stress in concentrated emulsion is about an order of magnitude lower than the one found for single drops in simple shear flow. The latter comparison shows that the drop breakup in concentrated emulsions is strongly facilitated by the interaction with neighboring drops, and that this effect cannot be captured by simple replacement of η_C by η_{EM} in the consideration.

The obtained results with foams showed that, similarly to emulsions, bubble breakup is much easier in foams, as compared to the breakup of isolated bubbles in sheared Newtonian fluid, at similar shear stress. Note that the viscosity ratio

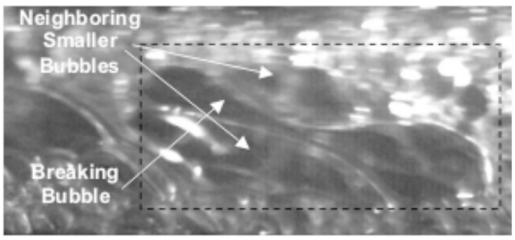

(a)

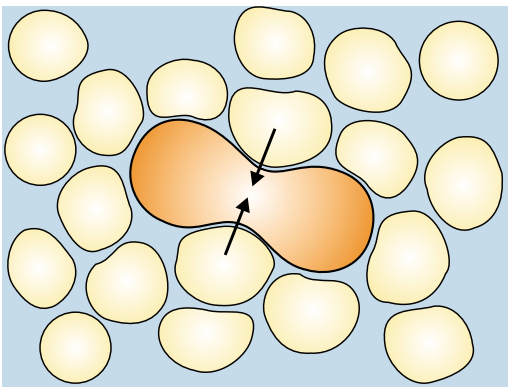

(b)

FIG. 8. (Color online) (a) Image of a breaking bubble in sheared foam, captured by a high-speed video camera. The foam was generated from soap solution, containing 40 wt % glycerol, $\Phi \approx 0.97$. The applied shear rate was 30 s^{-1}. (b) Schematic presentation of the breakage process in sheared foams and concentrated emulsions. The neighboring bubbles and drops press the thinnest middle part of the elongated "central" bubble and drop, thus creating capillary instability and facilitating the breakage. This "structural" effect is caused by the close confinement of the dispersed particles in such systems. Therefore we call it "structure-induced capillary instability" and it leads to significantly lower critical capillary numbers (critical shear stresses), as compared to those for single drops and bubbles.

for the bubbles in the studied foams is $\lambda \approx 10^{-4}$, which means that the critical capillary number for isolated bubbles would be $Ca_{CR} \sim 25$ [18,21], whereas experimentally we determined $Ca_{CR} \approx 0.4$ for foams. This huge difference in Ca_{CR} for isolated bubbles and for bubbles in concentrated foams, indicates that the mechanisms of bubble breakup in these two cases are rather different, which is mainly due to the irregular shear flow and the strong interaction between the bubbles in sheared foams, i.e., to the inherent microheterogeneous structure of foams at the length scale of bubble size.

Preliminary observations of the process of bubble breakup in sheared foams by high-speed camera (Redlake, MotionXtra, HG-100K System) indicated that the neighboring smaller bubbles facilitate the subdivision of the big bubbles mainly by pressing the middle (thinnest) portion of the elongated bubbles—see Fig. 8(a) for a camera image and Fig. 8(b) for a schematic presentation of this effect.

The fact that the replacement of η_C by η_{EM} in the consideration cannot explain the data by using the conventional "effective medium" approach [15] and optical observations like those illustrated in Fig. 8(a) indicate that the process of breakup in concentrated emulsions and foams is strongly affected by the local structure around the breaking drop and bubble, and does not comply with the rules of the classical capillary instability of single drops and bubbles. Thus we could conclude that another type of capillary instability, induced by drop and bubble interaction with their structured environment, is governing the subdivision of drops and bubbles in the systems studied. It seems appropriate to introduce the term "structure-induced capillary instability" to account for the effect of structured environment on drop and bubble breakup. Note that a qualitatively similar structure-induced instability could be expected in the presence of solid particles in the foam and emulsion, as well, which opens new possibilities for control of bubble and drop size. Further optical observations, combined with rheological measurements, are planned to clarify the details and the quantitative relations of this new type of capillary instability.

D. Relation between the viscous stress of the foams and emulsions and mean bubble and drop size after the fast process of breakup

Until now we focused the discussion on the critical stress, which causes bubble and drop breakup in sheared foam and emulsion. In the current section we shift the focus to the relation between the mean bubble and drop size and the shear stress, measured after completion of the process of fast breakup, when the system enters the period of relatively slow changes in the bubble and drop size. Thus we consider here relations, typical for the outcome of the fast breakup process in the studied foams and emulsions.

As explained in Sec. III F, after finishing the bubble and drop breaking experiments at fixed shear rate or stress, we measured the rheological properties of the obtained foams and emulsions. The rheological data can be represented as dimensionless total shear stress, $\tilde{\tau} = \tau R_{32}/\sigma$, or dimensionless viscous stress, $\tilde{\tau}_V = \tau_V R_{32}/\sigma$, vs the capillary number $Ca = (\eta_C \dot{\gamma} R_{32}/\sigma)$. The viscous stress was calculated after subtraction of the yield stress from the total stress, $\tau_V = \tau - \tau_0$. Note that we use the mean bubble and drop size R_{32} to define the dimensionless stresses in the current section, $\tilde{\tau}$, whereas we used the local bubble radius R in the preceding sections, to account for the different ratios between the average shear stress and the capillary pressures of the various bubbles in a given sample.

The analysis of the experimental results for the dependences of $\tilde{\tau}$ and $\tilde{\tau}_V$ on Ca showed that in the period, which follows the fast process of bubble and drop breakup, all studied foams and emulsions with $\Phi > 0.90$ exhibited similar dimensionless average viscous stress, $\tilde{\tau}_{ST} = \tau_V R_{32}/\sigma \approx 0.25$. (At $\Phi < 0.90$, the dimensionless stress noticeably decreased with the decrease of Φ.)

The above conclusion is illustrated with results from rheological measurements, shown in Fig. 8—note that all curves $\tilde{\tau}_V$(Ca) stop at $\tilde{\tau}_{ST} \approx 0.25$ when the shear rate (viz. the capillary number) in the rheological measurements becomes equal to the shear rate applied during the process of bubble and drop breakup (this corresponds to the uppermost points in the rheological curves shown in Fig. 9). On the other hand, as seen from Fig. 9, the capillary numbers corresponding to the

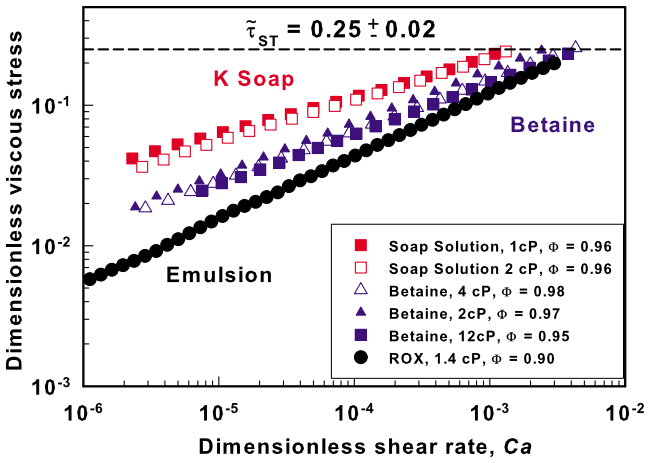

FIG. 9. (Color online) Dimensionless shear viscous stress ($\tau_V R_{32}/\sigma$) vs Ca for foams generated from 3 wt % CAPB solutions and from soap solutions of different viscosities, at different bubble volume fractions. Experimental results with emulsions stabilized by 3 wt % ROX solutions are also shown for comparison. The dimensionless viscous stress, corresponding to the shear rate used for bubble and drop breakup, is almost the same, $\tilde{\tau}_{ST} \approx 0.25$, for all these samples.

breakup process, Ca_{ST}, depend significantly on the specific experimental conditions (type of surfactant, Φ, etc.).

These results show reciprocal relation between the measured viscous stress and the mean bubble and drop size in all studied foams and concentrated emulsions with $\Phi \geq 90\%$, after completion of the fast process of breakup, $\tau_V \approx 0.25\sigma/R_{32}$, independently of the used surfactant, dispersed phase volume fraction, and viscosity of continuous phase. Whether this simple relation is applicable to higher viscosity ratios than those encountered in our study, $\lambda < 1$, remains to be seen in future studies.

V. CONCLUSIONS

We performed a systematic experimental study to clarify the conditions for bubble breakup in foams and drop breakup in concentrated emulsions. The bubble and drop breakup was accomplished between the plates of rotational rheometer, at fixed shear rate (or fixed shear stress). The kinetics of the process was followed by measuring the resulting shear stress (rate), and the bubble and drop size distributions were measured before and after completion of the breakup experiment. Surfactants with different surface modules were used and the viscosity of the continuous phase was varied to study the importance of these factors.

The obtained results could be summarized as follows:

Well defined critical shear stress exists, $\tilde{\tau}_{CR} = \tau_{CR} R/\sigma$, above which bubbles or drops of radius R break in sheared foam or concentrated emulsion. For foams stabilized with different surfactants, $\tilde{\tau}_{CR} \approx 0.40 \pm 0.02$, independently of the bubble volume fraction ($\Phi > 0.90$) and viscosity of the foaming solution. For hexadecane-in-water emulsions with $\Phi > 0.85$, the critical stress is $\tilde{\tau}_{CR} \approx 0.15 \pm 0.02$.

Fast bubble and drop breakup is observed (within several seconds) when more than 50% by volume of the bubbles and drops are subject to average shear stress, which is above the critical one, $\tilde{\tau}(R) = \tau R/\sigma > \tilde{\tau}_{CR}$. Slow breakup is observed (time scale of minutes and dozens of minutes) when 5–10 % of the bubbles and drops are subject to stress higher than the critical one. No breakup is observed when all bubbles and drops are under stress lower than $\tilde{\tau}_{CR}$.

After the period of fast breakup, a subsequent period of slow breakup is established, during which the viscous shear stress τ_{ST} and the mean bubble and drop size, R_{32}, are interrelated—for all foams and emulsions with $\Phi > 0.9$ studied, $\tau_{ST} R_{32}/\sigma \approx 0.25$.

The kinetics of breakup depends strongly on bubble polydispersity—faster breakup is observed in polydisperse foams, as compared to monodisperse foams (under equivalent all other conditions). Furthermore, a long induction period was observed (and explained) with sheared monodisperse foams, see Fig. 5. These results clearly show that the mean bubble size is insufficient to describe the kinetics of the breakup process and that the width of the size distribution is a very important factor for this process.

The most significant conclusion from the performed study is that the bubble breakup in foams is much easier, due to the interaction with the neighboring bubbles, as compared to the breakup of single bubbles in sheared Newtonian liquid; see Figs. 7 and 8. Indeed, the critical shear stress for bubble breakup in foams, $\tilde{\tau}_{CR} \approx 0.40$, is about two orders of magnitude lower than the respective critical stress for single bubbles. This strong effect of bubble-bubble interactions cannot be accounted for by simply replacing the viscosity of the continuous phase with the foam viscosity in the conventional analysis. A similar conclusion was reached for concentrated emulsions as well. This result is discussed in Sec. IV C in terms of a new type of capillary instability of the breaking drops and bubbles, which is governed by the local structure around them (structure-induced capillary instability, Figure 8). More refined theoretical and modeling approaches, which account for the local structure at the scale of the breaking bubbles and drops, are needed to explain the measured values of $\tilde{\tau}_{CR}$.

ACKNOWLEDGMENTS

This study was supported by Unilever R&D, Trumbull, CT, and by COST action P21 "Physics of Drops" of the ESF. The authors are grateful to Dr. N. Vankova for preparing the initial emulsions by membrane emulsification.

[1] H. M. Princen, in *Encyclopedia of Emulsion Technology*, edited by J. Sjöblom (Marcel Dekker, New York, 2001), Chap. 11, p. 243.
[2] *Foams: Theory, Measurements and Applications*, edited by R. K. Prud'homme and A. Khan (Marcel Dekker, New York, 1996).
[3] D. Exerowa and P. M. Kruglyakov, *Foams and Foam Films: Theory, Experiment, Application* (Elsevier, Amsterdam, 1998).
[4] S. A. Koehler, S. Hilgenfeldt, and H. A. Stone, Langmuir **16**, 6327 (2000).
[5] M. Durand, G. Martinoty, and D. Langevin, Phys. Rev. E **60**, R6307 (1999).
[6] O. Pitois, C. Fritz, and M. Vignes-Adler, J. Colloid Interface Sci. **282**, 458 (2005).
[7] A. Saint-Jalmes, Soft Matter **2**, 836 (2005).
[8] J. Lambert, I. Cantat, R. Delannay, R. Mokso, P. Cloetens, J. A. Glazier, and F. Graner, Phys. Rev. Lett. **99**, 058304 (2007).
[9] S. M. Bhavaraju, T. W. F. Russell, and H. W. Blanch, AIChE J. **24**, 454 (1978).
[10] J. F. Walter and H. W. Blanch, Chem. Eng. J. **32**, B7 (1986).
[11] C. Martinez-Bazan, J. L. Montanes, and J. C. Lasheras, J. Fluid Mech. **401**, 157 (1999).
[12] C. Martinez-Bazan, J. L. Montanes, and J. C. Lasheras, J. Fluid Mech. **401**, 183 (1999).
[13] T. G. Mason and J. Bibette, Phys. Rev. Lett. **77**, 3481 (1996).
[14] T. G. Mason and J. Bibette, Langmuir **13**, 4600 (1997).
[15] K. M. B. Jansen, W. G. M. Agterof, and J. Mellema, J. Rheol. **45**, 227 (2001).
[16] C. Mabille, F. Leal-Calderon, J. Bibette, and V. Schmitt, Europhys. Lett. **61**, 708 (2003).
[17] X. Zhao, J. Rheol. **51**, 367 (2007).
[18] J. M. Rallison, Annu. Rev. Fluid Mech. **16**, 45 (1984).
[19] H. A. Stone, Annu. Rev. Fluid Mech. **26**, 65 (1994).
[20] E. J. Hinch and A. Acrivos, J. Fluid Mech. **98**, 305 (1980).
[21] E. J. Hinch and A. Acrivos, J. Fluid Mech. **98**, 305 (1980).
[22] H. P. Grace, Chem. Eng. Commun. **14**, 225 (1982).
[23] S. Tanveer and G. L. Vasconcelos, Phys. Rev. Lett. **73**, 2845 (1994).
[24] P. Doshi, I. Cohen, W. W. Zhang, M. Siegel, P. Howell, O. Basaran, and S. R. Nagel, Science **302**, 1185 (2003).
[25] M. Hameed, M. Siegel, Y. N. Young, J. Li, M. R. Booty, and D. T. Papageorgiou, J. Fluid Mech. **594**, 307 (2008).
[26] G. I. Taylor, Proc. R. Soc. London, Ser. A **146**, 501 (1934).
[27] S. Tomotika, Proc. R. Soc. London, Ser. A **150**, 322 (1935).
[28] B. J. Bentley and L. G. Leal, J. Fluid Mech. **167**, 219 (1986).
[29] B. J. Bentley and L. G. Leal, J. Fluid Mech. **167**, 241 (1986).
[30] H. A. Stone, B. J. Bentley, and L. G. Leal, J. Fluid Mech. **173**, 131 (1986).
[31] H. A. Stone and L. G. Leal, J. Fluid Mech. **198**, 399 (1989).
[32] H. A. Stone and L. G. Leal, J. Fluid Mech. **206**, 223 (1989).
[33] H. A. Stone and L. G. Leal, J. Fluid Mech. **220**, 161 (1990).
[34] N. D. Denkov, V. Subraminian, D. Gurovich, and A. Lips, Colloids Surf., A **263**, 129 (2005).
[35] Y. T. Hu and A. Lips, J. Rheol. **45**, 1453 (2001).
[36] Y. T. Hu and A. Lips, J. Rheol. **47**, 349 (2003).
[37] Y. T. Hu and A. Lips, Phys. Rev. Lett. **91**, 044501 (2003).
[38] V. Sibillo, G. Pasquariello, M. Simeone, V. Cristini, and S. Guido, Phys. Rev. Lett. **97**, 054502 (2006).
[39] M. Loewenberg and E. J. Hinch, J. Fluid Mech. **321**, 395 (1996).
[40] C. Mabille, V. Schmitt, Ph. Gorria, F. Leal Calderon, V. Faye, B. Deminiere, and J. Bibette, Langmuir **16**, 422 (2000).
[41] N. D. Denkov, Langmuir **20**, 9463 (2004).
[42] N. C. Christov, D. N. Ganchev, N. D. Vassileva, N. D. Denkov, K. D. Danov, and P. A. Kralchevsky, Colloids Surf., A **209**, 83 (2002).
[43] K. Kandori, in *Food Processing: Recent Developments*, edited by A. G. Gaonkar (Elsveier, Amsterdam, 1995), pp. 113–142.
[44] P. R. Garrett, J. D. Hines, S. C. Joyce, and P. T. Whittal, Report prepared for Unilever R&D, Port Sunlight, 1993.
[45] W. S. Rasband and J. Image, U. S. National Institutes of Health, Bethesda, Maryland, USA, http://rsb.info.nih.gov/ij/, 1997–2006.
[46] P. S. Denkova, S. Tcholakova, N. D. Denkov, K. D. Danov, B. Campbell, C. Shawl, and D. Kim, Langmuir **20**, 11402 (2004).
[47] O. Sather, in *Encyclopedic Handbook of Emulsion Technology*, edited by J. Sjöblom (Dekker, New York, 2001), Chap. 15.